Journal of Sound and Vibration (1997) **201**(1), 23–41

NON-LINEAR VIBRATIONS OF A STRUCTURE CAUSED BY WATER SLOSHING IN A RECTANGULAR TANK

T. Ikeda and N. Nakagawa

Faculty of Engineering, *Hiroshima University*, 4-1, *Kagamiyama* 1-*chome*, *Higashi-Hiroshima*, *Hiroshima* 739, *Japan*

(*Received* 13 *September* 1994, *and in final form* 19 *August* 1996)

The non-linear vibrations of a structure coupled with water sloshing in a rectangular tank are theoretically and experimentally studied. The water tank is attached to a structure to suppress the horizontal vibrations of the structure caused by a sinusoidal excitation. In the theoretical analysis, considering the only source of non-linearity of the liquid inertia to be due to a large sloshing amplitude, the modal equations for sloshing are presented. Secondly, the solutions for the harmonic oscillations of the structure and the water surface are determined, including their stability analyses. Then, the resonance curves for this system are shown. As a result, the resonance curves are found to change from the soft spring type to the hard spring type as the water depth decreases. The resonance curves also show that a super-summed-and-differential harmonic oscillation can occur at the tuning frequency when the magnitude of excitation is comparatively large. This is a kind of non-linear forced oscillation due to the non-linearity of the fluid force. The appearance of this oscillation reduces the efficacy of vibration suppression by using the water tank. In conclusion, it was ascertained that these results agreed qualitatively well with the experimental results.

1. INTRODUCTION

Vibrations of a structure, coupled with the sloshing of the liquid surface, are seen in systems such as elevated water tanks, or storage tanks for LNG (Liquefied Natural Gas). Therefore, this kind of vibration is an important problem in industry. A device for the suppression of this vibration, called a TSD (i.e., Tuned Sloshing Damper), has been developed in order to control the vibration of a tower-like structure with a long period [1–3]. The effects of this device have already been verified experimentally, and the device has been applied to some practical structures [4–7]. The TSD is a kind of control device for vibration, having a function similar to that of a dynamic absorber, in which the fundamental natural frequency of sloshing in a liquid tank is tuned to the natural frequency of a structure in order to utilize the liquid force acting on the tank walls. Until now, the TSD has been studied experimentally. In order to investigate the behaviour of this kind of system precisely, one should consider the non-linearity of the fluid force, especially at resonance, when the magnitude of the fluid surface becomes marked.

Up to now, many papers have reported on the sloshing phenomena in a rigid rectangular tank. As for the non-linear response of the sloshing in a rectangular tank subjected horizontally to a sinusoidal excitation, there are analyses by means of the perturbation method, by Faltinsen [8] and Hayama *et al*. [9], research on the fluctuation of the hydraulic pressure, by Kimura *et al*. [10], and theoretical and experimental research by means of the

0022–460X/97/110023 + 19 $25.00/0/sv960722

shallow water wave theory, by Shimizu and Hayama [11], Lepelletier and Raichlen [12] and Ishibashi and Hayama [13]. Most of this research, such as that of Senda and Nakagawa [14] and Housner [15], which is concerned with the vibrations of structures with a TSD of the rectangular tank type, subjected to a sinusoidal excitation, deal with a linear system. There seem to be only a few reports on the coupled vibration of a structure and sloshing, in which the non-linearity of the fluid force due to sloshing is considered. For example, Fujino *et al*. [16], Ishikawa and Kaneko [17] and Kaneko [18] have presented resonance curves obtained by simulation via the method of finite differences, and discussed these in comparison with experimental results. The resonance curves have not been obtained theoretically, however, although, Ibrahim and Barr [19], Peterson [20] and Welt and Modi [21] have theoretically and experimentally investigated the non-linear vibrations of a structure with a TSD of cylindrical tank type, as have Sayar and Baumgarten [22] for one of spherical tank type.

This paper presents theoretical and experimental resonance curves for the horizontal motion of a structure to which a rectangular tank partially filled with water is attached, and which is subjected to a sinusoidal excitation. Here, the only source of non-linearity of the liquid inertia considered is that due to a large sloshing amplitude. In the theoretical analysis, the modal equations of motion are derived that govern the non-linear coupled vibration of the structure with the sloshing phenomenon. Then, the steady state solution for the harmonic oscillation is determined, its stability analysis is performed, and resonance curves are shown for various depths of water. From the numerical simulation, it is also found that there can occur a super-summed-and-differential harmonic oscillation near the tuning frequency when the excitation is comparatively large. This kind of non-linear forced oscillation becomes a serious obstacle for the vibration control of the structure in practical engineering systems. In experiments, quantitatively good agreement was obtained between the theoretical characteristics and the experimental results.

2. THEORETICAL ANALYSIS

2.1. EQUATIONS OF MOTION

The theoretical model is shown in Figure 1. A structure consisting of a cantilever beam and a mass m is horizontally subjected to a sinusoidal excitation. The rigid and rectangular tank, with a width d and a length l, partially filled with liquid to a depth h, is attached to the mass m. The moving co-ordinate system is considered, Oxy, which is fixed on the tank, and the x-axis of which coincides with the undisturbed water surface. The motion of the water is assumed to be possible in a two-dimensional plane; that is, in the x-y plane. The displacements of the structure and the water surface at the position x are x_1 and η, respectively. The equations of motion for the liquid motion have been derived in references

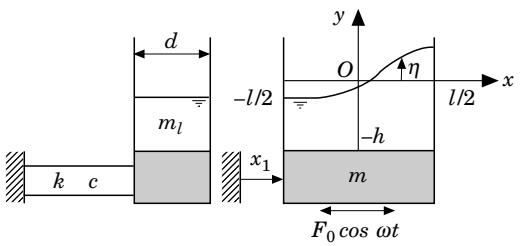

Figure 1. A model for theoretical analysis.

[19, 23]. The velocity potential for the relative motion of the liquid to the tank is ϕ. According to the references, the Laplace equation (or the continuity equation) is

$$\nabla^2\phi(x, y, t) \equiv \partial^2\phi/\partial x^2 + \partial^2\phi/\partial y^2 = 0, \tag{1}$$

and the Euler energy equation (or the pressure equation) is

$$\frac{\partial\phi}{\partial t} + \tfrac{1}{2}\left\{\left(\frac{\partial\phi}{\partial x}\right)^2 + \left(\frac{\partial\phi}{\partial y}\right)^2\right\} + gy + \frac{P}{\rho} - \tfrac{1}{2}\dot{x}_1^2 + \mu\phi = -\ddot{x}_1 x, \tag{2}$$

where $P(x, y, t)$ is the fluid pressure, μ is the viscosity, ρ is the density, and g is the acceleration due to gravity. Also, t is the time, and a superscript dot denotes differentiation with respect to time. In equation (2) the small viscosity term $\mu\phi$ takes account of all kinds of damping effects of the fluid; the fluid is assumed to obey a potential flow with a sufficient accuracy.

Here, we consider that the structure with a spring constant k and a damping coefficient c is subjected to the harmonic excitation $F_0 \cos \omega t$. The equation of motion for the structure is

$$m\ddot{x}_1 + c\dot{x}_1 + kx_1 = F_l + F_0 \cos \omega t. \tag{3}$$

According to reference [19], the longitudinal deflection of the cantilever beam yields non-linear terms in equation (3). However, as shown in Appendix A, these terms can be neglected, because they are negligibly small. In equation (3), F_l denotes the horizontal fluid force, which is applied on the side walls of the tank in the direction of x_1. F_l is given by

$$F_l = d\int_{-h}^{\eta_1} P(l/2, y, t)\,\mathrm{d}y - d\int_{-h}^{\eta_2} P(-l/2, y, t)\,\mathrm{d}y, \tag{4}$$

where η_1 and η_2 represent the surface elevations at the side walls; that is, at $x = l/2$ and $x = -l/2$, respectively. As shown in section 2.2, it will be seen that integrating equation (4) yields non-linear terms.

The following dimensionless quantities are introduced:

$$x_1' = x_1/l, \quad \eta' = \eta/l, \quad x' = x/l, \quad y' = y/l, \quad d' = \rho d l^2/M, \quad h' = h/l,$$

$$\phi' = \phi/(l^2 p_1), \quad v = m/M, \quad k' = k/(Mp_1^2), \quad c' = c/(Mp_1), \quad \mu' = \mu/p_1,$$

$$F_l' = F_l/(Mlp_1^2), \quad P' = P/(\rho l^2 p_1^2), \quad F_0' = F_0/(Mlp_1^2), \quad \lambda_1' = \lambda_1 l, \quad \lambda_2' = \lambda_2 l,$$

$$\omega' = \omega/p_1, \quad t' = p_1 t,$$

$$[M = m + m_l, \quad p_1 = \sqrt{g\lambda_1 \tanh(\lambda_1 h)}, \quad \lambda_1 = \pi/l, \quad \lambda_2 = 2\pi/l]. \tag{5}$$

Here the parameters in square brackets are dimensional quantities, and m_l denotes the mass of the fluid. In equation (5), λ_n are roots satisfying the characteristic equation

$$\sin(\lambda l) = 0. \tag{6}$$

The roots correspond to the natural frequencies of asymmetrical and symmetrical sloshing modes, designated as λ_{2n-1} and λ_{2n}, respectively. These are given by

$$\lambda_{2n-1} = (2n - 1)\pi/l, \quad \lambda_{2n} = 2n\pi/l, \quad n = 1, 2, 3, \ldots. \tag{7}$$

For example, the natural frequency p_1, which corresponds to an asymmetrical sloshing mode of the first order, can be determined by using λ_1. Equations (1)–(4) are rewritten in dimensionless form by using equations (5), as follows:

$$\phi_{xx} + \phi_{yy} = 0, \tag{8}$$

$$\phi_t + \tfrac{1}{2}(\phi_x^2 + \phi_y^2) + \frac{y}{\lambda_1 \tanh(\lambda_1 h)} + P - \tfrac{1}{2}\dot{x}_1^2 + \mu\phi = -\ddot{x}_1 x, \tag{9}$$

$$v\ddot{x}_1 + c\dot{x}_1 + kx_1 = F_l + F_0 \cos \omega t, \tag{10}$$

$$F_l = d\int_{-h}^{\eta_1} P(1/2, y, t)\,\mathrm{d}y - d\int_{-h}^{\eta_2} P(-1/2, y, t)\,\mathrm{d}y. \tag{11}$$

Here, and in what follows, the primes $'$ have been omitted. In equations (8) and (9), the subscripts t, x and y indicate partial derivation with respect to the respective variables.

The boundary conditions for the fluid velocities at the side and bottom walls are as follows:

$$\phi_x = 0 \quad \text{at } x = \pm 1/2, \qquad \phi_y = 0 \quad \text{at } y = -h. \tag{12a, b}$$

The vertical velocity of a fluid particle on the free surface must be the same as the vertical velocity of the free surface [9]. Therefore the following boundary condition is obtained:

$$\frac{\partial}{\partial t}\eta(x, t) = \phi_y - \phi_x \eta_x|_{y=\eta}. \tag{13}$$

In addition, since $P = 0$ at the free surface $y = \eta$, the boundary condition for equation (9) can be written

$$\phi_t + \tfrac{1}{2}(\phi_x^2 + \phi_y^2) + \frac{y}{\lambda_1 \tanh(\lambda_1 h)} - \tfrac{1}{2}\dot{x}_1^2 + \mu\phi|_{y=\eta} = -\ddot{x}_1 x. \tag{14}$$

2.2. MODAL EQUATIONS

First, the linear system which is governed by equation (8), and by equation (9) where the terms $\mu\phi$, $-\frac{1}{2}\dot{x}_1^2$, $-\ddot{x}_1 x$ and $\frac{1}{2}(\phi_x^2 + \phi_y^2)$ are excluded, is considered. The free vibrations of ϕ and η for the linear system can be solved in a series form by using the boundary conditions, where the non-linear terms are excluded from equations (12)–(14) [14]. Then, the solutions for the non-linear forced oscillations of ϕ and η are assumed to be given in terms of the asymmetrical and symmetrical sloshing modes, which are the same as eigenfunctions obtained in the linear analysis, as follows:

$$\phi(x, y, t) = \sum_{n=1}^{\infty} [a_{2n-1}(t) \sin(\lambda_{2n-1}x) \cosh\{\lambda_{2n-1}(y + h)\}/\cosh(\lambda_{2n-1}h)$$

$$+ a_{2n}(t) \cos(\lambda_{2n}x) \cosh\{\lambda_{2n}(y + h)\}/\cosh(\lambda_{2n}h)], \tag{15a}$$

$$\eta(x, t) = \sum_{n=1}^{\infty} \{b_{2n-1}(t) \sin(\lambda_{2n-1}x) + b_{2n}(t) \cos(\lambda_{2n}x)\}. \tag{15b}$$

Here a_i and b_i ($i = 1, 2, 3, \ldots$) are unknown functions of time.

One can expand x on the right side of equation (14) into a series of the same eigenfunctions as those in equation (15) as follows:

$$x = \sum_{n=1}^{\infty} \{S_{2n-1} \sin(\lambda_{2n-1}x) + S_{2n} \cos(\lambda_{2n}x)\},$$

$$S_{2n-1} = (-1)^{n+1}4/\{(2n-1)^2\pi^2\}, \qquad S_{2n} = 0. \tag{16}$$

Upon introducing the small parameter ϵ, and denoting the order of ϵ by $O(\epsilon)$, the orders of the quantities are assumed to be as follows [23, 24]:

$$a_1, b_1, x_1 \sim O(\varepsilon^{1/3}), \qquad a_2, b_2, c, \mu \sim O(\varepsilon^{2/3}), \qquad a_3, b_3, F_0 \sim O(\varepsilon^{3/3}). \tag{17}$$

In expressions (17), for expedience, the orders of the predominant variables x_1, a_1 and b_1 are assumed to be the same. Also, the orders of a_2 and b_2 are assumed to be smaller by $O(\varepsilon^{1/3})$ than those of a_1 and b_1. Furthermore, η is assumed to be small according to the assumption of equations (17). After expanding equations (13) and (14) in a Taylor series about $\eta = 0$, and substituting equations (15) and (16), one equates the coefficients of $\sin \lambda_1 x$ or $\cos \lambda_2 x$ on both sides of the resulting equations to an accuracy of $O(\varepsilon)$. In this way, and also with calculation of the integral for F_i in equation (10), one obtains the modal equations as follows:

$$\dot{a}_1 + \mu a_1 + Q_1 b_1 + Q_2 \ddot{x}_1 + Q_3 b_2 \dot{a}_1 + Q_4 b_1^2 \dot{a}_1 + Q_5 b_1 \dot{a}_2 + Q_6 a_1 a_2 + Q_7 a_1^2 b_1 = 0, \tag{18a}$$

$$\dot{a}_2 + Q_8 b_2 + Q_9 b_1 \dot{a}_1 + Q_{10} a_1^2 = 0, \tag{18b}$$

$$\dot{b}_1 + Q_{11} a_1 + Q_{12} a_1 b_2 + Q_{13} a_2 b_1 + Q_{14} a_1 b_1^2 = 0, \tag{18c}$$

$$\dot{b}_2 + Q_{15} a_2 + Q_{16} a_1 b_1 = 0, \tag{18d}$$

$$Q_{17}\ddot{x}_1 + c\dot{x}_1 + kx_1 + Q_{18}\dot{a}_1 + \mu Q_{19} a_1 + Q_{20} b_2 \dot{a}_1 + Q_{21} b_1^2 \dot{a}_1 + Q_{22} b_1 \dot{a}_2 + Q_{23} b_2 \ddot{x}_1 + Q_{24} b_1 \dot{x}_1^2 + Q_{25} a_1 a_2 + Q_{26} b_1 b_2 + Q_{27} a_1^2 b_1 = F_0 \cos \omega t. \tag{18e}$$

Here Q_i ($i = 1, \ldots, 27$) are as follows:

$$Q_1 = 1/(\lambda_1 \mathrm{Th}_1), \quad Q_2 = 4/\pi^2, \quad Q_3 = -\lambda_1 \mathrm{Th}_1/2, \quad Q_4 = 3\lambda_1^2/8,$$
$$Q_5 = -\lambda_2 \mathrm{Th}_2/2, \quad Q_6 = -\lambda_1\lambda_2(1 + \mathrm{Th}_1\mathrm{Th}_2)/2, \quad Q_7 = \lambda_1^3 \mathrm{Th}_1,$$
$$Q_8 = 1/(\lambda_1 \mathrm{Th}_1), \quad Q_9 = -\lambda_1 \mathrm{Th}_1/2, \quad Q_{10} = -\lambda_1^2(\mathrm{Th}_1^2 - 1)/4,$$
$$Q_{11} = -\lambda_1 \mathrm{Th}_1, \quad Q_{12} = \lambda_1(\lambda_1 - \lambda_2)/2, \quad Q_{13} = -\lambda_2(\lambda_1 - \lambda_2)/2,$$
$$Q_{14} = -\lambda_1^3 \mathrm{Th}_1/8, \quad Q_{15} = -\lambda_2 \mathrm{Th}_2, \quad Q_{16} = \lambda_1^2, \quad Q_{17} = v + dh,$$
$$Q_{18} = 2d \mathrm{Th}_1/\lambda_1, \quad Q_{19} = 2d \mathrm{Th}_1/\lambda_1, \quad Q_{20} = -2d, \quad Q_{21} = d\lambda_1 \mathrm{Th}_1,$$
$$Q_{22} = -2d, \quad Q_{23} = -d, \quad Q_{24} = -d, \quad Q_{25} = d\lambda_2(\mathrm{Sh}_1 - \mathrm{Sh}_{31}/3)/(\mathrm{Ch}_1\mathrm{Ch}_2),$$
$$Q_{26} = -2d/(\lambda_1 \mathrm{Th}_1), \quad Q_{27} = d\lambda_1^2(\mathrm{Ch}_{21} - 1)/(2\mathrm{Ch}_1^2),$$
$$[\mathrm{Th}_1 = \tanh(\lambda_1 h), \quad \mathrm{Th}_2 = \tanh(\lambda_2 h), \quad \mathrm{Sh}_1 = \sinh(\lambda_1 h), \quad \mathrm{Sh}_{31} = \sinh(3\lambda_1 h),$$
$$\mathrm{Ch}_1 = \cosh(\lambda_1 h), \quad \mathrm{Ch}_2 = \cosh(\lambda_2 h), \quad \mathrm{Ch}_{21} = \cosh(2\lambda_1 h)]. \tag{19}$$

The equations for a_3 and b_3 are omitted in equations (18), because they are meaningless within the accuracy of $O(\varepsilon)$. Equations (18) are ordinary differential equations for the unknown functions of time a_i and b_i ($i = 1, 2$) and x_i. Therefore, by integrating this equation numerically, one can obtained a time history, as shown in Figure 2 of section 3.

Next, one considers the following equations, in which the damping terms, the excitation term and non-linear terms are excluded from equations (18), in order to determine the natural frequencies of the system:

$$\dot{a}_1 + Q_1 b_1 + Q_2 \ddot{x}_1 = 0, \qquad \dot{b}_1 + Q_{11} a_1 = 0, \qquad Q_{17} \ddot{x}_1 + k x_1 + Q_{18} \dot{a}_1 = 0. \tag{20}$$

Eliminating a_1 from equation (20), and using the relation $Q_1 Q_{11} = -1$ in equation (19), one obtains

$$Q_2 Q_{11} \ddot{x}_1 - \dddot{b}_1 - b_1 = 0, \qquad Q_{11} Q_{17} \ddot{x}_1 - Q_{18} \dddot{b}_1 + k Q_{11} x_1 = 0. \tag{21}$$

The solutions for the free vibration equations (21) are assumed in the forms

$$x_1 = A_1 \cos(qt + \beta), \qquad b_1 = A_2 \cos(qt + \beta). \tag{22}$$

By substituting equations (22) into equations (21), and setting the determinant of the coefficient matrix to zero, one obtains the frequency equation. Then, the natural frequencies q_1 and q_2 ($q_1 < q_2$) are given by

$$q_1^2, q_2^2 = \frac{1}{2(Q_2 Q_{18} - Q_{17})} \{ -(k + Q_{17}) \pm \sqrt{(k + Q_{17})^2 + 4k(Q_2 Q_{18} - Q_{17})} \}. \tag{23}$$

2.3. RESONANCE CURVES FOR THE HARMONIC OSCILLATIONS

To investigate the solutions of a harmonic oscillation for the linearized system of equations (18), the linearized system is expressed by equations (20), where $F_0 \cos \omega t$ is added to the third equation. Thus the solutions of forced oscillations for a_i, b_i and x_1 include explicitly the only the frequency ω. However, since equation (18) is non-linear, substituting the terms of frequency ω into equations (18) yields terms of other frequencies. Accordingly, these terms need to be added into the solutions of forced oscillations in equation (18). For example, since the existence of the term $Q_7 a_1^2 b_1$ in equation (18a) yields a component of frequency 3ω, this component must be added into the solutions for a_1, b_1 and x_1. Similarly, a component of frequency 2ω must be included in the solution for a_2 due to the term $Q_{10} a_1^2$ in equation (18b). However, an alternative approach can be adopted here, based on the harmonic balance method. According to the FFT spectrum (see Figure 3 of section 3) from the numerical time history of equations (18), one can assume the solutions of a_i, b_i ($i = 1, 2$) and x_1 to be of the following forms:

$$\begin{aligned} a_1 &= u_1 \cos \omega t - v_1 \sin \omega t + w_1 \cos 3\omega t - z_1 \sin 3\omega t, \\ b_1 &= u_2 \cos \omega t - v_2 \sin \omega t + w_2 \cos 3\omega t - z_2 \sin 3\omega t, \\ x_1 &= u_3 \cos \omega t - v_3 \sin \omega t + w_3 \cos 3\omega t - z_3 \sin 3\omega t, \\ a_2 &= e_1 \cos 2\omega t - f_1 \sin 2\omega t, \qquad b_2 = e_2 \cos 2\omega t - f_2 \sin 2\omega t + r_0. \end{aligned} \tag{24}$$

Here the amplitudes u_i, v_i, w_i, z_i, e_j and f_j ($i = 1, 2, 3$; $j = 1, 2$), and the constant term r_0, are assumed to be slowly varying functions of time, and their orders of magnitude are in proportion to those of a_i, b_i ($i = 1, 2$) and x_1. Every time the amplitudes are differentiated with respect to time, their orders are assumed to decrease by $O(\varepsilon^{2/3})$ as follows:

$$\begin{gathered} u_i, v_i \sim O(\varepsilon^{1/3}), \qquad w_i, z_i, e_j, f_j, r_0 \sim O(\varepsilon^{2/3}), \qquad \dot{u}_i, \dot{v}_i \sim O(\varepsilon^{3/3}), \\ \dot{w}_i, \dot{z}_i, \dot{e}_j, \dot{f}_j, \dot{r}_0, \dot{r}_2 \sim O(\varepsilon^{4/3}), \qquad \ddot{u}_i, \ddot{v}_i \sim O(\varepsilon^{5/3}), \qquad \ddot{w}_i, \ddot{z}_i, \ddot{e}_j, \ddot{f}_j, \ddot{r}_0 \sim O(\varepsilon^{6/3}). \end{gathered} \tag{25}$$

Substituting equations (24) into equations (18), setting the coefficients of the terms of frequencies ω, 2ω and 3ω and the constant term to zero under the assumptions of expressions (25), one obtains

$$\dot{u}_1 - 2Q_2\omega\dot{v}_3 = -\mu u_1 + \omega v_1 - Q_1 u_2 + Q_2\omega^2 u_3 + g_1(u_j, v_j, e_j, f_j, r_0), \tag{26a}$$

$$\dot{v}_1 + 2Q_2\omega\dot{u}_3 = -\omega u_1 - \mu v_1 - Q_1 v_2 + Q_2\omega^2 v_3 + g_2(u_j, v_j, e_j, f_j, r_0), \tag{26b}$$

$$\dot{u}_2 = -Q_{11}u_1 + \omega v_2 + g_3(u_j, v_j, e_j, f_j, r_0), \tag{26c}$$

$$\dot{v}_2 = -Q_{11}v_1 - \omega u_2 + g_4(u_j, v_j, e_j, f_j, r_0), \tag{26d}$$

$$Q_{18}\dot{u}_1 - 2Q_{17}\omega\dot{v}_3 = -\mu Q_{19}u_1 + Q_{18}\omega v_1 - (k - Q_{17}\omega^2)u_3 + c\omega v_3 + F_0 + g_5(u_i, v_i, e_j, f_j, r_0), \tag{26e}$$

$$Q_{18}\dot{v}_1 + 2Q_{17}\omega\dot{u}_3 = -Q_{18}\omega u_1 - \mu Q_{19}v_1 - c\omega u_3 - (k - Q_{17}\omega^2)v_3 + g_6(u_i, v_i, e_j, f_j, r_0), \tag{26f}$$

$$-3\omega z_1 + Q_1 w_2 - 9Q_2\omega^2 w_3 = g_7(u_j, v_j, e_j, f_j), \tag{26g}$$

$$3\omega w_1 + Q_1 z_2 - 9Q_2\omega^2 z_3 = g_8(u_j, v_j, e_j, f_j), \tag{26h}$$

$$Q_{11}w_1 - 3\omega z_2 = g_9(u_j, v_j, e_j, f_j), \qquad Q_{11}z_1 + 3\omega w_2 = g_{10}(u_j, v_j, e_j, f_j), \tag{26i, j}$$

$$-3Q_{18}\omega z_1 + (k - 9Q_{17}\omega^2)w_3 = g_{11}(u_i, v_i, e_j, f_j), \tag{26k}$$

$$3Q_{18}\omega w_1 + (k - 9Q_{17}\omega^2)z_3 = g_{12}(u_i, v_i, e_j, f_j), \tag{26l}$$

$$e_1 = g_{13}(u_j, v_j, w_i, z_i), \qquad f_1 = g_{14}(u_j, v_j, w_i, z_i), \tag{26m, n}$$

$$e_2 = g_{15}(u_j, v_j, w_i, z_i), \qquad f_2 = g_{16}(u_j, v_j, w_i, z_i), \qquad r_0 = g_{17}(u_j, v_j) \tag{26o–q}$$

where $i = 1, 2, 3$ and $j = 1, 2$. The explicit expressions for equations (26) are shown in Appendix B. The functions g_k ($k = 1, 2, \ldots, 17$) on the right sides of equations (26) are the non-linear terms, which consist of the variables in the brackets. For example, the symbol u_i means that u_1, u_2 and u_3 are involved. The corresponding relationship between equations (18) and (26) is shown in Table 1. For example, Table 1 implies that equation (26b) can be derived from the coefficient of $\sin\omega t$ after substituting equation (24) into equation (18a). From equations (26), with $\dot{u}_i = 0$ and $\dot{v}_i = 0$, the steady state solutions can be calculated by a numerical method. The stability analysis can be also performed by introducing small deviations from the steady state solutions [25].

The procedure for the stability analysis is as follows. First, let the small deviations from the steady state solutions for (u_i, v_i, w_i, z_i) $(i = 1, 2, 3)$, (e_j, f_j) $(j = 1, 2)$ and r_0 be $(\xi_i, \eta_i, \gamma_i, \delta_i)$, (ρ_j, σ_j) and ζ, respectively. One has the matrix forms

$$\mathbf{X} = (\rho_1 \quad \sigma_1 \quad \rho_2 \quad \sigma_2 \quad \zeta)^{\mathrm{T}}, \qquad \mathbf{Y} = (\gamma_1 \quad \delta_1 \quad \gamma_2 \quad \delta_2 \quad \gamma_3 \quad \delta_3)^{\mathrm{T}},$$
$$\mathbf{Z} = (\xi_1 \quad \eta_1 \quad \xi_2 \quad \eta_2 \quad \xi_3 \quad \eta_3)^{\mathrm{T}}, \tag{27}$$

TABLE 1

Corresponding relationships between equations (18) *and* (26)

Equations	$\cos\omega t$			$\sin\omega t$			$\cos 3\omega t$			$\sin 3\omega t$			$\cos 2\omega t$		$\sin 2\omega t$		Constant
(18)	a	c	e	a	c	e	a	c	e	a	c	e	b	d	b	d	b
(26)	a	c	e	b	d	f	g	i	k	h	j	l	m, n, o, p				q

where **X**, **Y** and **Z** are the column vectors, and the superscript T denotes the transpose of the matrix in question. After giving these small deviations in the vicinity of the steady state solutions for equations (26), one expands the resulting equations in Taylor series about the steady state solutions. Then, one neglects all terms containing the second and higher powers of these small deviations. Using the equations for the steady state solutions in equations (26), one obtains

$$\dot{\mathbf{Z}} = \mathbf{AZ} + \mathbf{BX}, \qquad \mathbf{X} = \mathbf{CZ} + \mathbf{DY}, \qquad \mathbf{Y} = \mathbf{EZ} + \mathbf{FX}, \tag{28}$$

where **A**, **B**, etc., are matrices which can be determined from the coefficients of equations (26). By eliminating **X** and **Y** in equations (28), one obtains

$$\dot{\mathbf{Z}} = \mathbf{GZ}, \tag{29}$$

where

$$\mathbf{G} = \mathbf{A} + \mathbf{B}(\mathbf{I} - \mathbf{DF})^{-1}(\mathbf{C} + \mathbf{DE}), \tag{30}$$

and **I** is the unit matrix. Therefore, the stability analysis of the steady state solutions is related to the eigenvalue problem for the differential equation (29): namely, the steady state solution is stable when the real part of the eigenvalue for the matrix **G** is equal to or less than zero, and it is unstable when the real part is positive.

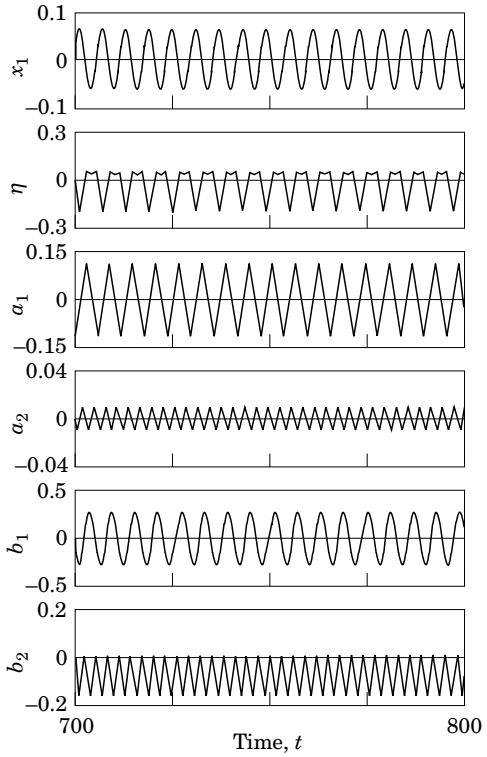

Figure 2. Steady state time histories when $v = 0{\cdot}94$, $k = 1{\cdot}0$, $c = 0{\cdot}013$, $\mu = 0{\cdot}024$, $h = 0{\cdot}6$, $d = 0{\cdot}1$, $F_0 = 0{\cdot}0015$, $x = 0{\cdot}15$ and $\omega = 1{\cdot}06$.

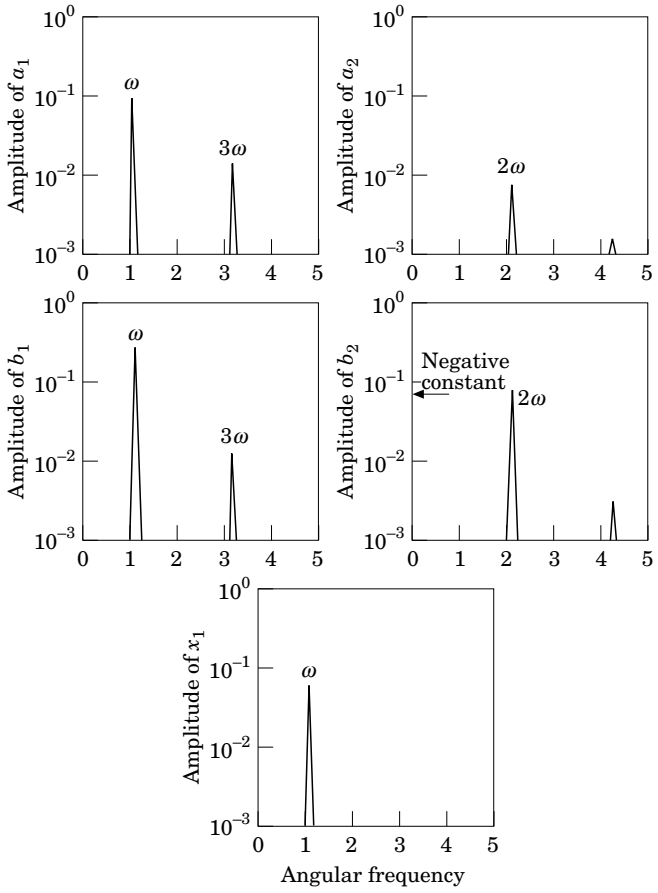

Figure 3. FFT spectra for the waveforms of Figure 2.

Now, one considers the system in which the water is assumed to be unmovable and the water mass is added to the structure mass. The equation of motion for this system is obtained by setting a_i and b_i $(i = 1, 2)$ in equation (18e) to zero, as follows:

$$Q_{17}\ddot{x}_1 + c\dot{x}_1 + kx_1 = F_0 \cos \omega t. \tag{31}$$

The resonance curve for equation (31) is given by

$$R = F_0/\sqrt{(k - Q_{17}\omega^2)^2 + c^2\omega^2}, \tag{32}$$

where R is an amplitude of the main system, and Q_{17} is given in equations (19).

3. NUMERICAL RESULTS

For the results to be presented, the values of the parameters were selected under a tuned condition such that the natural frequency of the main system is equal to the natural frequency p_1 corresponding to the first asymmetrical sloshing mode. Therefore, the relation $\sqrt{k/Q_{17}} = p_1 = 1$ holds in a dimensionless form.

In Figure 2 is shown the steady state time history obtained by the digital simulation of equations (18). The values of the parameters are $v = 0{\cdot}94$, $k = 1{\cdot}0$, $c = 0{\cdot}013$, $\mu = 0{\cdot}024$, $h = 0{\cdot}6$, $d = 0{\cdot}1$, $F_0 = 0{\cdot}0015$, $x = 0{\cdot}15$ and $\omega = 1{\cdot}06$. The system resonates at this value

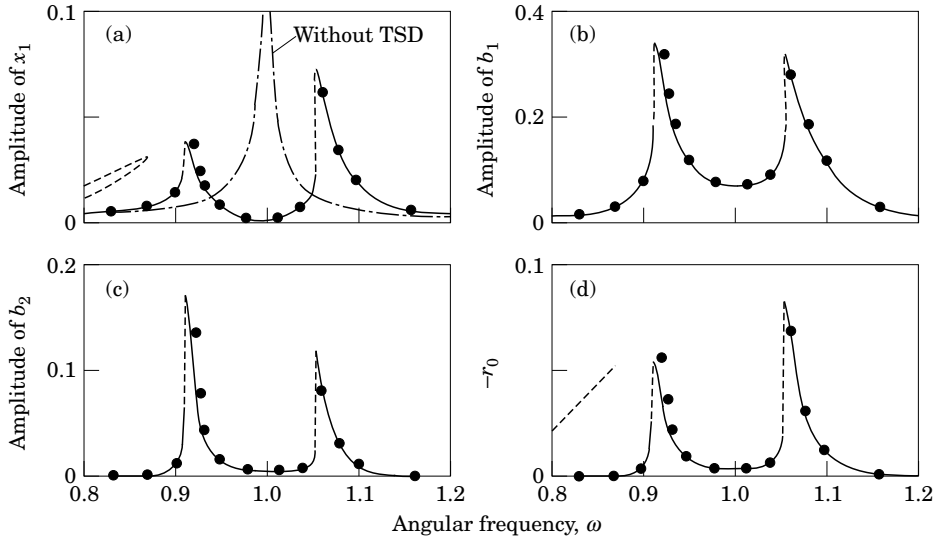

Figure 4. Theoretical resonance curves in the same case as for Figure 2 (i.e., for $h = 0{\cdot}06$). (a) The amplitude of the ω component in x_1; (b) the amplitude of the ω component in b_1; (c) the amplitude of the 2ω component in b_2; (d) the amplitude $-r_0$ of the constant component in b_2. ——, Stable; – – –, unstable; ●, simulation; TSD, Tuned Sloshing Damper.

of ω, and thus the amplitudes of the response become large (see Figure 4). In the simulation, the initial values at $t = 0$ are selected as $x_1 = 0{\cdot}01$, with the other values equal to zero. The time history of η is obtained by substituting the data for b_1 and b_2 into equations (15).

In Figure 3 are shown the FFT spectra from the time histories in Figure 2. For example, it can be seen from Figure 3 that there are dominant peaks of frequencies ω and 3ω in b_1, 2ω and the constant component (which should be noticed to be negative) in b_2, and ω in x_1. These results validate the assumption of the solution forms given in equations (24).

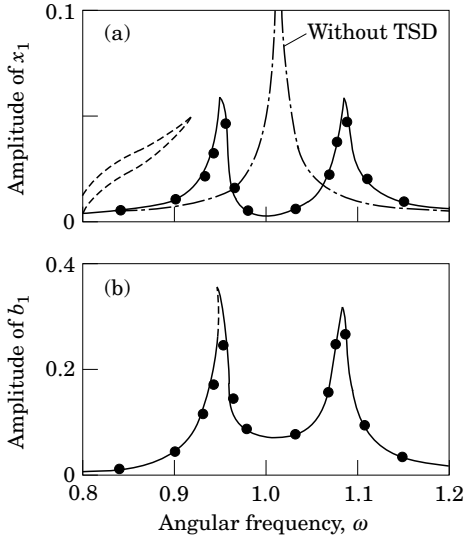

Figure 5. As Figure 4, but for $h = 0{\cdot}33$. (a) The amplitude of the ω component in x_1; (b) the amplitude of the ω component in b_1. ——, Stable; – – –, unstable; ●, simulation; TSD, Tuned Sloshing Damper.

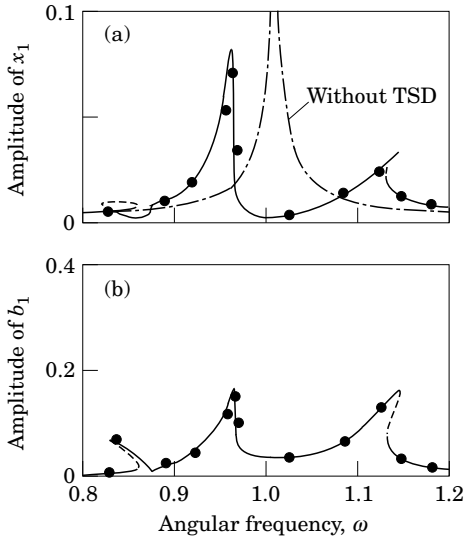

Figure 6. As Figure 4, but for $h = 0{\cdot}2$ and $d = 0{\cdot}2$. (a) The amplitude of the ω component in x_1; (b) the amplitude of the ω component in b_1. ——, Stable; – – –, unstable; ●, simulation; TSD, Tuned Sloshing Damper.

It is also indicated in Figure 3 that the maximum amplitude of b_2 is slightly larger than that of x_1. This seems inconsistent with assumptions (17). However, it is evident that the approximate solutions based on expressions (17) have a higher accuracy than those in the case assumed, as $x_1 = O(\varepsilon^{2/3})$.

In Figure 4 are shown the resonance curves for the component of ω (i.e., $\sqrt{u_3^2 + v_3^2}$) in x_1, the component of ω (i.e., $\sqrt{u_2^2 + v_2^2}$) in b_1, the component of 2ω (i.e., $\sqrt{e_2^2 + f_2^2}$) in b_2, and the constant component $-r_0$, which can be calculated from equations (26). The solid and broken lines represent the stable and unstable steady state solutions, respectively. The chain line denotes the resonance curve for the main system according to equation (32): that is, the resonance curve without a TSD (Tuned Sloshing Damper). The values of the parameter are the same as those for Figure 2. The shape of resonance curves is a soft spring type. The symbol "●" denotes the amplitude of the component of each frequency obtained by the FFT analysis of the time histories. Therefore, the theoretical resonance curve agree well with the results from the digital simulation. Also it is found that the peak for the main

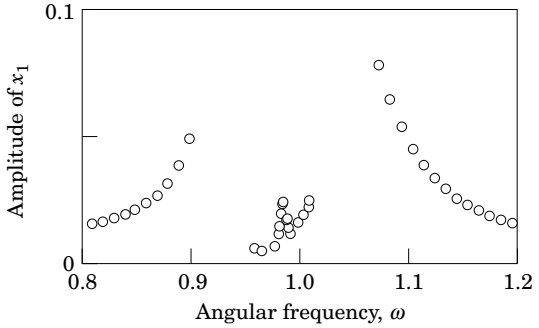

Figure 7. The theoretical resonance curve for x_1 obtained by digital simulation when the value of F_0 for Figure 4 is changed to 0·005. ○, Simulation.

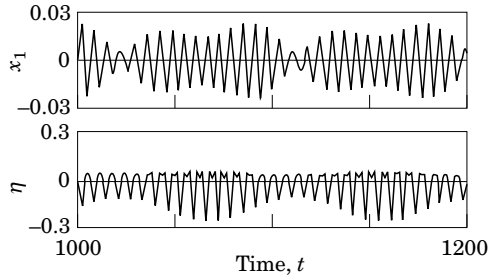

Figure 8. Steady state time histories of x_1 and η at $\omega = 0{\cdot}985$ in Figure 7.

system near $\omega \simeq 1$ vanishes by using a TSD, and that a TSD has the similar effect of vibration control to a dynamic absorber.

In Figures 5 and 6 are shown the resonance curves for water depths different from that in Figure 4. For Figure 5, $h = 0{\cdot}33$. For Figure 6, $h = 0{\cdot}2$ and $d = 0{\cdot}2$. The other parameters have the same values as those for Figure 4. Good agreement is shown in these figures between the theoretical curves and the simulation results. It is found from these figures that the resonance curves change from soft spring types to hard spring types as the water depth decreases.

In Figure 7 is shown the resonance curve of x_1 given by digital simulations in the case in which only the magnitude of the excitation is changed, from $F_0 = 0{\cdot}0015$ for Figure 4 to $F_0 = 0{\cdot}005$. The symbol "○" denotes the maximum amplitude obtained from the time history. The peak can be seen to be near $\omega = 1{\cdot}0$, which indicates the tuning frequency between the structure and the sloshing. In utilizing the water tank as the vibration absorber for a practical structure, this peak may becomes an obstacle.

In Figure 8 are shown the steady state time histories of x_1 and η at $\omega = 0{\cdot}985$ for Figure 7, and the FFT spectrum for x_1 for Figure 8 is shown in Figure 9. In this case, the natural frequencies of the system are $q_1 = 0{\cdot}930$ and $q_2 = 1{\cdot}089$ which can be calculated from equations (23). These two frequencies, except for ω ($=0{\cdot}985$) in Figure 9, are denoted by ω_1 ($=0{\cdot}917$ and ω_2 ($=1{\cdot}053$). These frequencies are close to the natural frequencies, and the relation

$$\omega_1 + \omega_2 = 2\omega \tag{33}$$

holds. Therefore, the oscillation in Figure 8 is a super-summed-and-differential harmonic oscillation [26], which is a kind of non-linear forced oscillation.

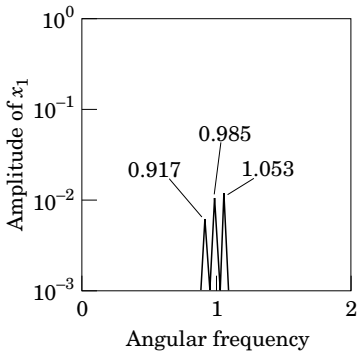

Figure 9. The FFT spectrum for x_1 in Figure 8.

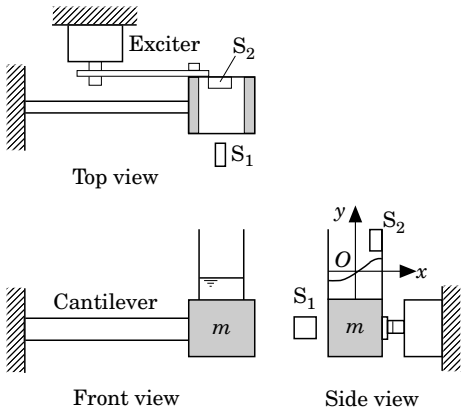

Figure 10. The experimental apparatus.

4. EXPERIMENTAL APPARATUS AND RESULTS

A schematic diagram of the experimental apparatus is shown in Figure 10. The mass m with the rectangular tank made of acrylic plastics was mounted at the end of the cantilever (the width and thickness of which were 50·0 mm and 3·1 mm, respectively). The mass m was sinusoidally excited through a thin aluminium plate by an electromagnetic exciter. The displacement x_1 of the mass m (i.e., the structure) and the elevation η of the water surface at the position of $x = 15$ mm were measured by the laser sensors S_1 and S_2. In the experiments, as shown in Table 2, three kinds of apparatus were used with mainly different water depths, and were called apparatuses A, B and C. In Table 2, the equivalent mass of the cantilever is included in the value of m, and the equivalent stiffness of the aluminium plate is contained in the value of k. The value of μ was measured from the waveforms of the free vibrations for the water surface. The value of μ for apparatus C was taken as the same value as that for apparatus B, becuase it could not be measured due to the disturbance of the water surface. The magnitude of excitation F_0 was calculated from the spring constant of the aluminium plate and the stroke of the exciter head when the mass m was fixed. In experiments, a water solution with white watercolors of 0·28% was used in order that the light of the laser could be reflected on the liquid surface. Each apparatus was constructed so that the natural frequency of the main system

TABLE 2

The dimensions of apparatuses A, B *and* C

	A	B	C
Structure mass, m (kg)	6·080	6·470	6·797
Spring constant, k (N/m)	1890	1513	921
Damping coefficient, c (Ns/m)	1·109	0·761	0·630
Tank length, l (m)	0·10	0·10	0·12
Tank width, d (m)	0·06	0·06	0·085
Water depth, h (m)	0·06	0·03	0·02
Water mass, m_l (kg)	0·367	0·183	0·205
Viscosity, μ (1/s)	0·40	0·60	—†
Force, F_0 (N)	0·205	0·139	0·152
Natural frequency, p_0 (Hz)	2·725	2·400	1·825

† The corresponding value could not be measured.

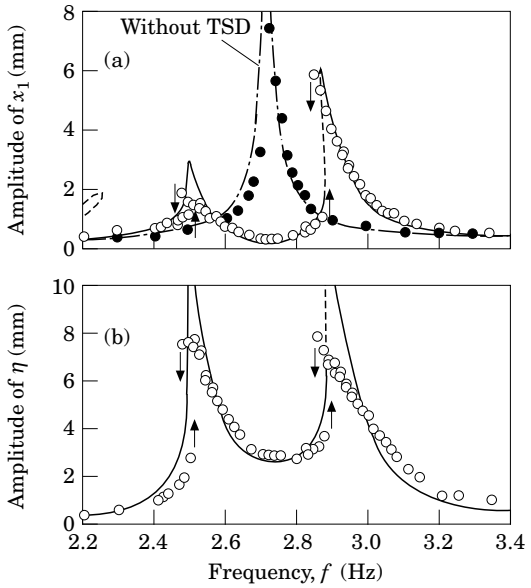

Figure 11. A comparison of the theoretical and experimental resonance curves for apparatus A when $h = 60$ mm. (a) Amplitudes of x_1; (b) amplitudes of η. ——, Stable solution of theoretical resonance curve; – – –, unstable solution of theoretical curve; ○, experiment for the case with TSD; ●, experiment for the case without TSD; ↑↓, jump phenomena.

$p_0 = (1/2\pi)\sqrt{k/M}$ Hz (where $M = m + m_l$) was equal to the natural frequency p_1 corresponding to the asymmetrical first mode of sloshing.

In Figures 11(a) and 11(b) are shown the resonance curves for the structure and the water surface for apparatus A, respectively. The abscissa of these figures is the excitation frequency f Hz. The solid and broken lines are the theoretical resonance curves for the system with a TSD, and the chain line is that for the system without a TSD (from equation (32)). These curves are of the same kinds as those in Figure 4. The symbol "○" denotes the maximum amplitude of the experimental waveform of x_1 and η for the system with a TSD, and the symbol "●" denotes the maximum amplitude of x_1 for the system without a TSD. The arrows denote the jump phenomena in the amplitude. The peak for the

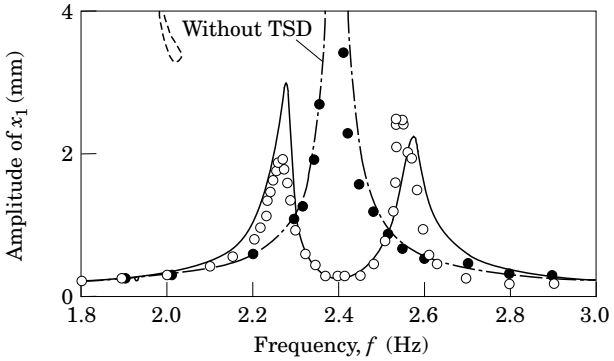

Figure 12. A comparison of the theoretical and experimental resonance curves for x_1 for apparatus B when $h = 30$ mm. ——, Stable solution of theoretical resonance curve; – – –, unstable solution of theoretical curve; ○, experiment for the case with TSD; ●, experiment for the case without TSD.

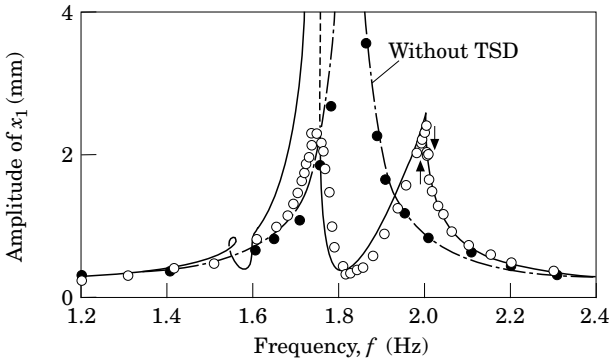

Figure 13. A comparison of the theoretical and experimental resonance curves for x_1 for apparatus C when $h = 20$ mm. ——, Stable solution of theoretical resonance curve; ——, unstable solution of theoretical curve; ○, experiment for the case with TSD; ●, experiment for the case without TSD; ↑↓, jump phenomena.

structure plotted by "●" near $f \simeq p_0$ was about 18 mm. The shape of this resonance curve is of a soft spring type. It is shown in Figure 11 that the theoretical curves agree well with the experimental results.

In Figures 12 and 13 are shown the resonance curves for the structure for apparatuses B and C, respectively. The peaks of the structure without a TSD near $f \simeq p_0$ were about 21 mm for apparatus B, and about 30 mm for apparatus C. The shape of the resonance curve for apparatus C is of a hard spring type. Also obtained were the experimental resonance curves shown in Figures 11–13, which are similar to the theoretical ones in Figures 4–6, respectively. Accordingly, also in the experiments, the resonance curve changed from a soft spring type to a hard spring type as the water depth decreased.

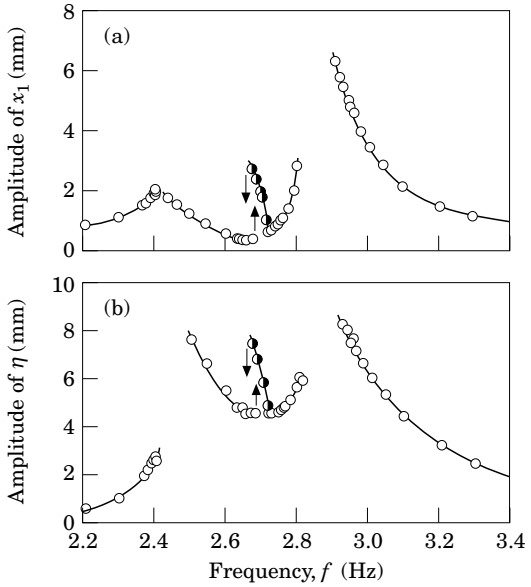

Figure 14. The experimental resonance curves for x_1 for apparatus A when $F_0 = 0{\cdot}64$ N. (a) Amplitudes of x_1; (b) amplitudes of η. —○—, Harmonics; —◑—, super-summed-and-differential harmonic oscillations; ↑↓, jump phenomena.

In Figure 14 is shown the experimental resonance curve for the structure for an apparatus similar to apparatus A when the magnitude of excitation ($F_0 = 0{\cdot}64$ N) was larger than that for Figure 11. In Figure 14, there is a peak denoted by the symbol "◑" near the tuning frequency ($f \simeq 2{\cdot}7$ Hz). In this case, the natural frequencies of this apparatus were f_1 ($=2{\cdot}48$ Hz) and f_2 ($=2{\cdot}93$ Hz). Considering that the two frequencies of this peak measured were close to f_1 and f_2, and that the relation $f_1 + f_2 \simeq 2f$ holds, one can see that this peak corresponds to the super-summed-and-differential harmonic oscillations. These experimental results mentioned above agreed well with the theoretical predictions.

5. CONCLUSIONS

The non-linear harmonic responses of the structure and the water surface in the rectangular tank have been theoretically and experimentally considered. The results can be summarized as follows.

(1) The modal equations, which are needed to analyze the non-linear coupled vibration of the structure with the sloshing, can be obtained.

(2) Depending on the water depth, the shapes of the resonance curves for the structure become soft spring types for a deep depth, and hard spring types for a shallow depth.

(3) When the magnitude of excitation is small, the amplitude of the structure becomes infinitesimal near the tuning frequency.

(4) If the magnitude of excitation is comparatively large, a super-summed-and-differential harmonic oscillation may occur near the tuning frequency.

(5) The validity of the theoretical analysis was confirmed by the experiments.

REFERENCES

1. V. J. Modi and F. Welt 1987 *Proceedings of International Conference on Flow Induced Vibrations*, 369–376. Vibration control using nutation dampers.
2. T. Miyata, H. Yamada and Y. Saitoh 1988 *Transactions of the Japan Society of Civil Engineers* (in Japanese) **34A**, 617–626. Suppression of tower-like structures vibration by damping effect of sloshing water contained.
3. T. Miyata, H. Yamada and Y. Saitoh 1989 *Transactions of the Japan Society of Civil Engineers* (in Japanese) **35A**, 553–560. Feasibility study of the sloshing damper system using rectangular containers.
4. H. Hagiuda 1989 *Mitsui Zosen Technical Review* (in Japanese) **137**, 13–20. Oscillation control system exploiting fluid force generated by water sloshing.
5. T. Noji, H. Yoshida, E. Tatsumi, H. Kosaka and H. Hagiuda 1990 *Journal of Structural and Construction Engineering*, *AIJ* (in Japanese) **411**, 97–105. Study of water-sloshing vibration control damper, part 1: hydrodynamic force characteristics of the device and damping effect of the system.
6. T. Ueda, R. Nakagaki, K. Koshida, K. Arima and H. Kado 1991 *The Hitachi Zosen Technical Review* (in Japanese) **52**(1), 25–30. Suppression of wind-induced vibration by dynamic dampers in tower-like structures.
7. Steel Structure and Civil Engineering Division 1991 *Mitsui Zosen Technical Review* (in Japanese) **143**, 17–25. Oscillation control of pylon and cables in cable stayed "Sakitama" Bridge (up-route side).
8. O. M. Faltinsen 1974 *Journal of Ship Research* **18**(4), 224–241. A nonlinear theory of sloshing in rectangular tanks.
9. S. Hayama, K. Aruga and T. Watanabe 1983 *Bulletin of the Japan Society of Mechanical Engineers*, **26**(219), 1641–1648. Nonlinear responses of sloshing in rectangular tanks (1st report, Nonlinear responses of surface elevation).
10. N. Kimura, H. Ohashi and M. Ikenouchi 1975 *Preprint of the Japan Society of Mechanical Engineers* (in Japanese) **750**(4), 93–96. A discussion on nonlinear responses of sloshing.

11. T. Shimizu and S. Hayama 1987 *Transactions of the Japan Society of Mechanical Engineers* (in Japanese) **53**(486)C, 357–363. Nonlinear response of sloshing based on the shallow water wave theory (1st report, Derivation of basic equations and nonlinear response in rectangular tanks).
12. T. G. Lepelletier and F. Raichlen 1988 *Journal of Engineering Mechanics* **114**(1), 1–23. Nonlinear oscillations in rectangular tanks.
13. H. Ishibashi and S. Hayama 1989 *Transactions of the Japan Society of Mechanical Engineers* (in Japanese) **55**(511)C, 663–670. Nonlinear response of sloshing based on the shallow water wave theory (2nd report, Nonlinear response in rectangular tanks and cylindrical tanks).
14. K. Senda and K. Nakagawa 1954 *Technical Reports of Osaka University* **4**(117), 247–264. On the vibration of an elevated water-tank—I.
15. G. W. Housner 1963 in *Nuclear Reactors and Earthquakes*, *TID*-7024, *U.S. Atomic Energy Commission*. See Chapter 6, pp. 183–209. Dynamic pressure on fluid containers.
16. Y. Fujino, B. M. Pacheco, Li-Min Sun, P. Chaiseri and M. Isobe 1989 *Transactions of the Japan Society of Civil Engineers* (in Japanese) **35A**, 561–574. Simulation of nonlinear waves in rectangular tuned liquid damper (TLD) and its verification.
17. M. Ishikawa and S. Kaneko 1991 *Preprint of the Japan Society of Mechanical Engineers* (in Japanese) **910**(39)B, 243–248. A study on the damper for structures utilizing the resonance of fluid in a tank.
18. S. Kaneko 1992 *Journal of the Marine Engineering Society in Japan* (in Japanese) **27**(4), 323–329. Dampers for structures utilizing the resonance of fluid in a tank.
19. R. A. Ibrahim 1975 *Journal of Sound and Vibration* **42**, 159–179. Autoparametric resonance in a structure containing a liquid, part I: two mode interaction.
20. L. D. Peterson 1989 *American Institute of Aeronautics and Astronautics Journal* **27**(9), 1230–1240. Nonlinear fluid slosh coupled to the dynamics of a spacecraft.
21. F. Welt and V. J. Moji 1992 *Transactions of the American Society of Mechanical Engineers*, *Journal of Vibration and Acoustics* **114**(1), 10–16. Vibration damping through liquid sloshing, part I: a nonlinear analysis.
22. B. A. Sayar and J. R. Baumgarten 1982 *American Institute of Aeronautics and Astronautics Journal* **20**(11), 1534–1538. Linear and nonlinear analysis of fluid slosh dampers.
23. M. Sakata, K. Kimura and M. Utsumi 1984 *Journal of Sound and Vibration* **94**, 351–363. Non-stationary response of non-linear liquid motion in a cylindrical tank subjected to random base excitation.
24. R. E. Hutton 1963 *NASA Technical Note*, D-1870, 1–64. An investigation of resonant, nonlinear, nonplanar free surface oscillations of a fluid.
25. T. Yamamoto and S. Hayashi 1963 *Bulletin of the Japan Society of Mechanical Engineers* **6**(23), 420–429. On the response curves and the stability of summed-and-differential harmonic oscillations.
26. T. Yamamoto, K. Yasuda and T. Nagoh 1975 *Bulletin of the Japan Society of Mechanical Engineers* **18**(128), 1082–1089. Super-division harmonic oscillations in a nonlinear multidegree-of-freedom system.

APPENDIX A

According to reference [19], the longitudinal deflection δ of the cantilever beam yields the following non-linear terms in the equation of motion (3), written in a dimensionless form,

$$(36m_l/25L^2)x_1(x_1\ddot{x}_1 + \dot{x}_1^2) \quad [\equiv A], \tag{A1}$$

where L is the length of the cantilever, and m_l is the mass of liquid. By using the dimensionless quantities defined by equations (5), this term can be rewritten in dimensionless form as

$$\tfrac{36}{25}d'h'(l/L)^2x_1'(x_1'\ddot{x}_1' + \dot{x}_1'^2) \quad [\equiv A']. \tag{A2}$$

It seems that this term should be added in equation (10). However, since the width of the tank was $l = 100$ mm and the length of the cantilever L was equal to 350 mm

in the experimental apparatus, the relation $l/L < 1$ held. Here, as one assumes $x_1 = O(\epsilon^{1/3})$,

$$A' < O(\epsilon^{3/3}) = O(\epsilon) \tag{A3}$$

holds. Therefore, the term A or A' can be neglected by considering that equation (18e) is derived to an accuracy of $O(\epsilon)$.

APPENDIX B

The complete expressions for equations (26) are as follows:

$$\begin{aligned}\dot{u}_1 - 2Q_2\omega\dot{v}_3 = &-\mu u_1 + \omega v_1 - Q_1 u_2 + Q_2\omega^2 u_3 \\ &+ \tfrac{1}{4}Q_4\omega\{v_1(3u_2^2 + v_2^2) - 2u_1u_2v_2\} - \tfrac{1}{4}Q_7\{u_2(3u_1^2 + v_1^2) + 2u_1v_1v_2\} \\ &- (Q_5\omega v_2 + \tfrac{1}{2}Q_6u_1)e_1 + (Q_5\omega u_2 - \tfrac{1}{2}Q_6v_1)f_1 \\ &+ \tfrac{1}{2}Q_3\omega(v_1e_2 - u_1f_2) + Q_3\omega v_1 r_0,\end{aligned} \tag{B1}$$

$$\begin{aligned}\dot{v}_1 - 2Q_2\omega\dot{u}_3 = &-\omega u_1 - \mu v_1 - Q_1 v_2 + Q_2\omega^2 v_3 \\ &+ \tfrac{1}{4}Q_4\omega\{u_1(u_2^2 + 3v_2^2) - 2u_2v_1v_2\} - \tfrac{1}{4}Q_7\{v_2(u_1^2 + 3v_1^2) + 2u_1u_2v_1\} \\ &- (Q_5\omega u_2 - \tfrac{1}{2}Q_6v_1)e_1 - (Q_5\omega v_2 + \tfrac{1}{2}Q_6u_1)f_1 \\ &+ \tfrac{1}{2}Q_3\omega(u_1e_2 + v_1f_2) - Q_3\omega u_1 r_0,\end{aligned} \tag{B2}$$

$$\begin{aligned}\dot{u}_2 = &-Q_{11}u_1 + \omega v_2 - \tfrac{1}{4}Q_{14}\{u_1(3u_2^2 + v_2^2) + 2u_2v_1v_2\} \\ &- \tfrac{1}{2}Q_{13}(u_2e_1 + v_2f_1) - \tfrac{1}{2}Q_{12}(u_1e_2 + v_1f_2) - Q_{12}u_1r_0,\end{aligned} \tag{B3}$$

$$\begin{aligned}\dot{v}_2 = &-Q_{11}v_1 - \omega u_2 - \tfrac{1}{4}Q_{14}\{v_1(u_2^2 + 3v_2^2) + 2u_1u_2v_2\} \\ &+ \tfrac{1}{2}Q_{13}(v_2e_1 - u_2f_1) + \tfrac{1}{2}Q_{12}(v_1e_2 - u_1f_2) - Q_{12}v_1r_0,\end{aligned} \tag{B4}$$

$$\begin{aligned}Q_{18}\dot{u}_1 - 2Q_{17}\omega\dot{v}_3 = &-\mu Q_{19}u_1 + Q_{18}\omega v_1 - (k - Q_{17}\omega^2)u_3 + c\omega v_3 \\ &+ \tfrac{1}{4}Q_{21}\omega\{v_1(3u_2^2 + v_2^2) - 2u_1u_2v_2\} - \tfrac{1}{4}Q_{24}\omega^2\{u_2(u_3^2 + 3v_3^2) - 2u_3v_2v_3\} \\ &- \tfrac{1}{4}Q_{27}\{u_2(3u_1^2 + v_1^2) + 2u_1v_1v_2\} - (Q_{22}\omega v_2 + \tfrac{1}{2}Q_{25}u_1)e_1 \\ &+ (Q_{22}\omega u_2 - \tfrac{1}{2}Q_{25}v_1)f_1 + \tfrac{1}{2}(Q_{20}\omega v_1 + Q_{23}\omega^2 u_3 - Q_{26}u_2)e_2 \\ &- \tfrac{1}{2}(Q_{20}\omega u_1 - Q_{23}\omega^2 v_3 + Q_{26}v_2)f_2 \\ &+ (Q_{20}\omega v_1 + Q_{23}\omega^2 u_3 - Q_{26}u_2)r_0 + F_0,\end{aligned} \tag{B5}$$

$$\begin{aligned}Q_{18}\dot{v}_1 + 2Q_{17}\omega\dot{u}_3 = &-Q_{18}\omega u_1 - \mu Q_{19}v_1 - c\omega u_3 - (k - Q_{17}\omega^2)v_3 \\ &- \tfrac{1}{4}Q_{21}\omega\{u_1\{u_2^2 + 3v_2^2) - 2u_2v_1v_2\} - \tfrac{1}{4}Q_{24}\omega^2\{v_2(3u_3^2 + v_3^2) - 2u_2u_3v_3\} \\ &- \tfrac{1}{4}Q_{27}\{v_2(u_1^2 + 3v_1^2) + 2u_1u_2v_1\} - (Q_{22}\omega u_2 - \tfrac{1}{2}Q_{25}v_1)e_1 \\ &- (Q_{22}\omega v_2 + \tfrac{1}{2}Q_{25}u_1)f_1 + \tfrac{1}{2}(Q_{20}\omega u_1 - Q_{23}\omega^2 v_3 + Q_{26}v_2)e_2 \\ &+ \tfrac{1}{2}(Q_{20}\omega v_1 + Q_{23}\omega^2 u_3 - Q_{26}u_2)f_2 - (Q_{20}\omega u_1 - Q_{23}\omega^2 v_3 \\ &+ Q_{26}v_2)r_0,\end{aligned} \tag{B6}$$

$$-3\omega z_1 + Q_1 w_2 - 9Q_2\omega^2 w_3 = \tfrac{1}{4}Q_4\omega\{v_1(u_2^2 - v_2^2) + 2u_1u_2v_2\} - \tfrac{1}{4}Q_7\{u_2(u_1^2 - v_1^2) - 2u_1v_1v_2\} + (Q_5\omega v_2 - \tfrac{1}{2}Q_6u_1)e_1 + (Q_5\omega u_2 + \tfrac{1}{2}Q_6v_1)f_1 + Q_3\omega(u_1f_2 + v_1e_2), \tag{B7}$$

$$3\omega w_1 + Q_1 z_2 - 9Q_2\omega^2 z_3 = -\tfrac{1}{4}Q_4\omega\{u_1(u_2^2 - v_2^2) - 2u_2v_1v_2\} - \tfrac{1}{4}Q_7\{v_2(u_1^2 - v_1^2) + 2u_1u_2v_1\} - (Q_5\omega u_2 + \tfrac{1}{2}Q_6v_1)e_1 + (Q_5\omega v_2 - \tfrac{1}{2}Q_6u_1)f_1 - \tfrac{1}{2}Q_3\omega(u_1e_2 - v_1f_2), \tag{B8}$$

$$Q_{11}w_1 - 3\omega z_2 = -\tfrac{1}{4}Q_{14}\{u_1(u_2^2 - v_2^2) - 2u_2v_1v_2\} - \tfrac{1}{2}Q_{13}(u_2e_1 - v_2f_1) - \tfrac{1}{2}Q_{12}(u_1e_2 - v_1f_2), \tag{B9}$$

$$Q_{11}z_1 + 3\omega w_2 = -\tfrac{1}{4}Q_{14}\{v_1(u_2^2 - v_2^2) + 2u_1u_2v_2\} - \tfrac{1}{2}Q_{13}(v_2e_1 + u_2f_1) - \tfrac{1}{2}Q_{12}(v_1e_2 + u_1f_2), \tag{B10}$$

$$-3Q_{18}\omega z_1 + (k - 9Q_{17}\omega^2)w_3 = \tfrac{1}{4}Q_{21}\omega\{v_1(u_2^2 - v_2^2) + 2u_1u_2v_2\} + \tfrac{1}{4}Q_{24}\omega^2\{u_2(u_3^2 - v_3^2) - 2u_3v_2v_3\} - \tfrac{1}{4}Q_{27}\{u_2(u_1^2 - v_1^2) - 2u_1v_1v_2\} + (Q_{22}\omega v_2 - \tfrac{1}{2}Q_{25}u_1)e_1 + (Q_{22}\omega u_2 + \tfrac{1}{2}Q_{25}v_1)f_1 + \tfrac{1}{2}(Q_{20}\omega v_1 + Q_{23}\omega^2u_3 - Q_{26}u_2)e_2 + \tfrac{1}{2}(Q_{20}\omega u_1 - Q_{23}\omega^2v_3 + Q_{26}v_2)f_2, \tag{B11}$$

$$3Q_{18}\omega w_1 + (k - 9Q_{17}\omega^2)z_3 = -\tfrac{1}{4}Q_{21}\omega\{u_1(u_2^2 - v_2^2) - 2u_2v_1v_2\} + \tfrac{1}{4}Q_{24}\omega^2\{v_2(u_3^2 - v_3^2) + 2u_2u_3v_3\} - \tfrac{1}{4}Q_{27}\{v_2(u_1^2 - v_1^2) + 2u_1u_2v_1\} - (Q_{22}\omega u_2 + \tfrac{1}{2}Q_{25}v_1)e_1 + (Q_{22}\omega v_2 - \tfrac{1}{2}Q_{25}u_1)f_1 - \tfrac{1}{2}(Q_{20}\omega u_1 - Q_{23}\omega^2v_3 + Q_{26}v_2)e_2 + \tfrac{1}{2}(Q_{20}\omega v_1 + Q_{23}\omega^2u_3 - Q_{26}u_2)f_2, \tag{B12}$$

$$e_1 = -\{Q_9\omega^2(u_1u_2 - u_1w_2 + 3u_2w_1 - v_1v_2 - v_1z_2 + 3v_2z_1) + 2Q_{10} - \omega(u_1v_1 + u_1z_1 - v_1w_1) + \tfrac{1}{2}Q_8Q_{16}(u_1u_2 + u_1w_2 + u_2w_1 - v_1v_2 + v_1z_2 + v_2z_1)\}/(4\omega^2 + Q_8Q_{15}), \tag{B13}$$

$$f_1 = -\{Q_9\omega^2(u_1v_2 - u_1z_2 + u_2v_1 + 3u_2z_1 + v_1w_2 - 3v_2w_1) - Q_{10}\omega(u_1^2 - v_1^2 + 2u_1w_1 + 2v_1z_1) + \tfrac{1}{2}Q_8Q_{16}(u_1v_2 + u_1z_2 + u_2v_1 + u_2z_1 - v_1w_2 - v_2w_1)\}/(4\omega^2 + Q_8Q_{15}), \tag{B14}$$

$$e_2 = \{\tfrac{1}{2}Q_9Q_{15}\omega(u_1v_2 - u_1z_2 + u_2v_1 + 3u_2z_1 + v_1w_2 - 3v_2w_1) - \tfrac{1}{2}Q_{10}Q_{15}(u_1^2 - v_1^2 + 2u_1w_1 + 2v_1z_1) - Q_{16}\omega(u_1v_2 + u_1z_2 + u_2v_1 + u_2z_1 - v_1w_2 - v_2w_1)\}/(4\omega^2 + Q_8Q_{15}), \tag{B15}$$

$$f_2 = -\{\tfrac{1}{2}Q_9Q_{15}\omega(u_1u_2 - u_1w_2 + 3u_2w_1 - v_1v_2 - v_1z_2 + 3v_2z_1) + Q_{10}Q_{15}(u_1v_1 + u_1z_1 - v_1w_1) - Q_{16}\omega(u_1u_2 + u_1w_2 + u_2w_1 - v_1v_2 + v_1z_2 + v_2z_1)\}/(4\omega^2 + Q_8Q_{15}), \tag{B16}$$

$$r_0 = -\{Q_9\omega(u_1v_2 - u_2v_1) + Q_{10}(u_1^2 + v_1^2)\}/(2Q_8). \tag{B17}$$